(*S*)-5-(2′-fluorophenyl)-*N,N*-dimethyl-1,2,3,4-tetrahydronaphthalen-2-amine, a serotonin receptor modulator, possesses anticonvulsant, prosocial, and anxiolytic-like properties in an *Fmr1* knockout mouse model of fragile X syndrome and autism spectrum disorder

Jessica L. Armstrong[a], *Austen B. Casey*[b], *Tanishka S. Saraf*[a], *Munmun Mukherjee*[b], *Raymond G. Booth*[b], *Clinton E. Canal*[a*]

[a] Department of Pharmaceutical Sciences, College of Pharmacy, Mercer University Health Sciences Center, Mercer University, Atlanta, GA 30341, USA

[b] Center for Drug Discovery, Department of Pharmaceutical Sciences, and Department of Chemistry and Chemical Biology, Northeastern University, Boston, MA 02131 USA

SUPPORTING INFORMATION

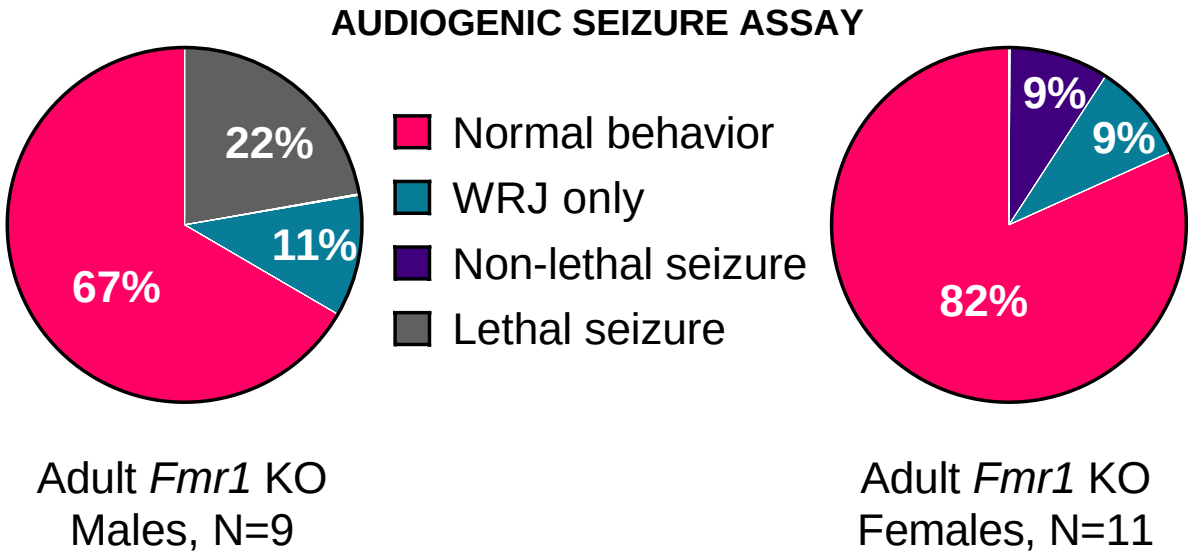

Figure S1. Audiogenic seizure prevalence in adult (>P60) *Fmr1* knockout (KO) mice after vehicle treatment. Most (78% of male and 91% of female) adult *Fmr1* KO mice did not display audiogenic seizures when pretreated with vehicle. There was not a significant difference in the occurrence of audiogenic seizures between adult male (left) and female (right) *Fmr1* KO mice.

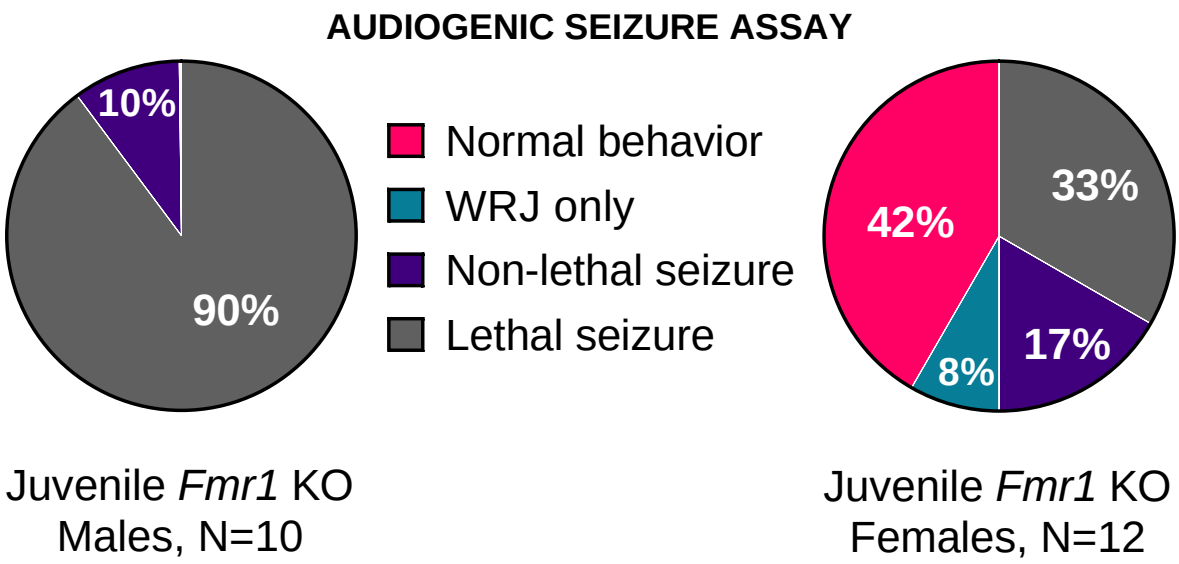

Figure S2. Sex difference in audiogenic seizure susceptibility in juvenile *Fmr1* knockout (KO) mice. Juvenile males (left) exhibited increased susceptibility to audiogenic seizures compared to juvenile females (right). 100% of vehicle-treated males experienced seizures with 90% dying from respiratory arrest. 50% of vehicle-treated females experienced seizures with 33% dying from respiratory arrest. Of the 50% of vehicle-treated females that did not exhibit seizures, 42% showed normal behavior and 8% showed only WRJ behavior.

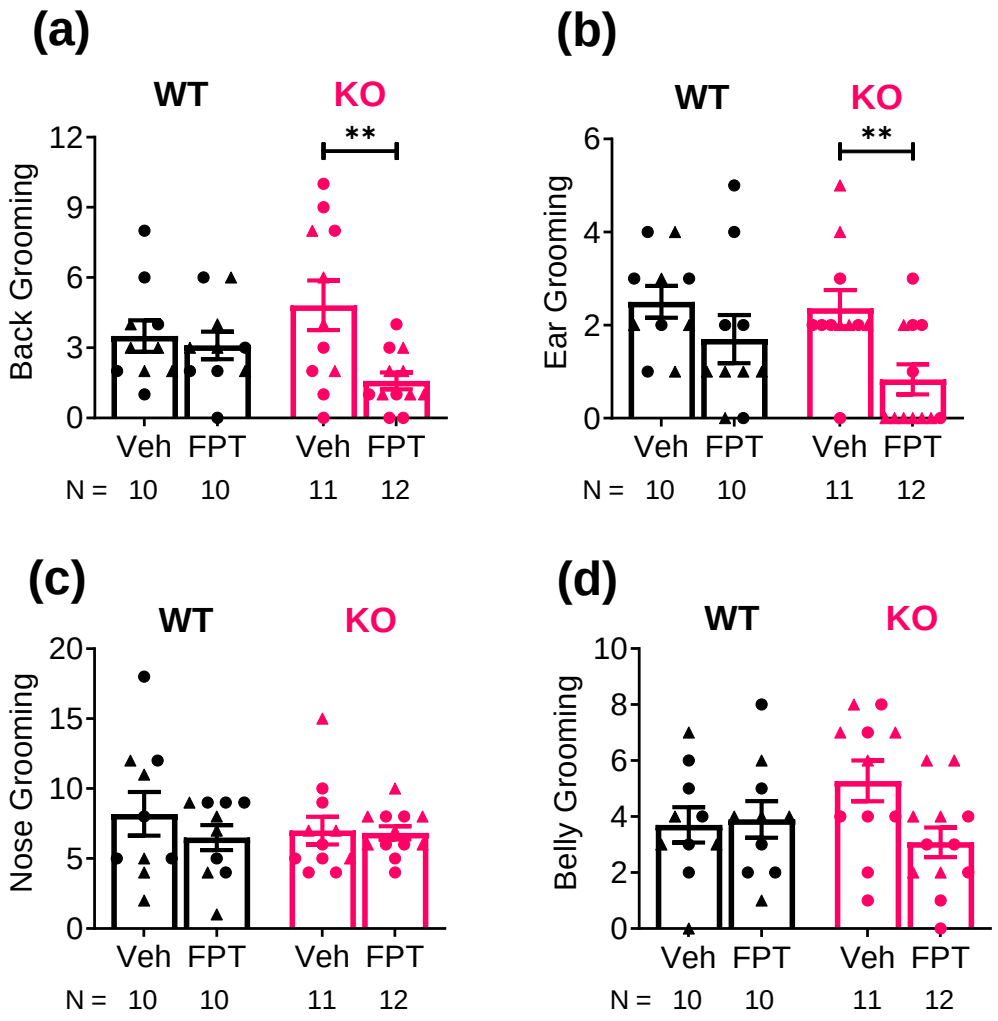

Figure S3. Effects of FPT on grooming of distinct body parts in wild-type (WT) and *Fmr1* knockout (KO) mice. **(a)** Bouts that involved back grooming, **(b)** ear grooming, **(c)** nose grooming, and **(d)** belly grooming; KO mice showed a trend towards increased belly grooming relative to WT type mice. FPT significantly reduced back and ear grooming selectively in KO mice.

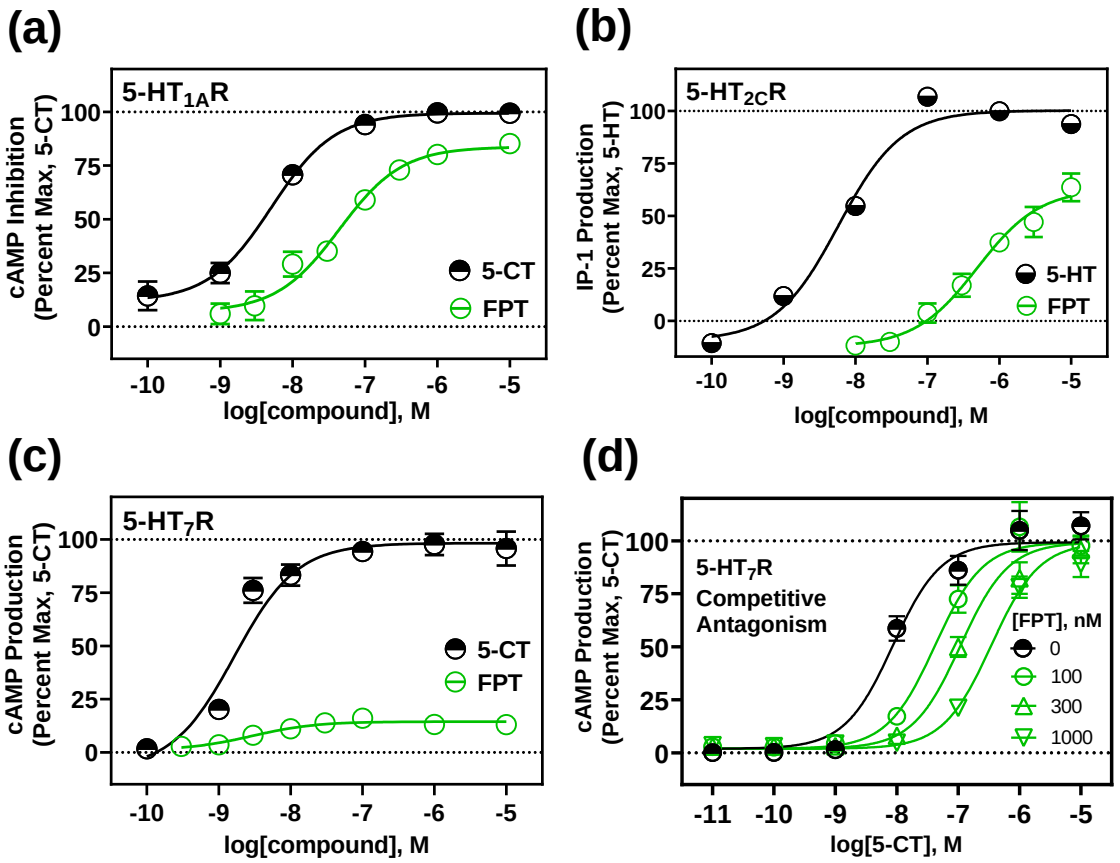

Figure S4. In vitro functional activity of FPT compared to reference full agonists at 5-HT$_{1A}$Rs, 5-HT$_{2C}$Rs, and 5-HT$_{7}$Rs. **(a)** FPT behaved as a high efficacy partial agonist at 5-HT$_{1A}$Rs, **(b)** high efficacy partial agonist at 5-HT$_{2C}$Rs, and **(c)** low efficacy partial agonist at 5-HT$_{7}$Rs. **(d)** FPT competitively antagonized the response of the full agonist 5-CT at 5-HT$_{7}$Rs, without attenuating E$_{MAX}$. Efficacy was normalized to the % maximal response of reference agonists 5-CT or 5-HT.

Table S1. Expression of c-Fos (c-Fos+ cell counts per mm^2) in wild-type (WT) and *Fmr1* knockout (KO) mice after treatment with vehicle or FPT. Data shown are means (±SEM), and % change is FPT-treated relative to vehicle-treated.

Brain Region	WT Veh	WT FPT	% Change	KO Veh	KO FPT	% Change
BLAa	242 (59)	623 (165)	157% (93)	303 (81)	1011 (215)	234%* (115)
BLAv	175 (45)	262 (69)	50% (55)	168 (15)	413 (188)	146% (114)
BLAp	273 (53)	355 (55)	30% (32)	284 (60)	728 (213)	156% (93)
DG	128 (29)	101 (15)	-21% (21)	75 (10)	162 (58)	116% (83)
CA1	163 (61)	113 (33)	-31% (33)	83 (17)	122 (34)	47% (50)
CA3	252 (94)	259 (43)	3% (42)	258 (28)	348 (126)	35% (51)
SS cortex	965 (315)	1095 (493)	14% (63)	582 (138)	1224 (379)	110% (82)
Pvi, PH, DMH	420 (95)	298 (75)	-29% (24)	285 (33)	437 (175)	53% (64)
RSpV	605 (351)	465 (185)	-23% (54)	316 (68)	556 (121)	76% (54)

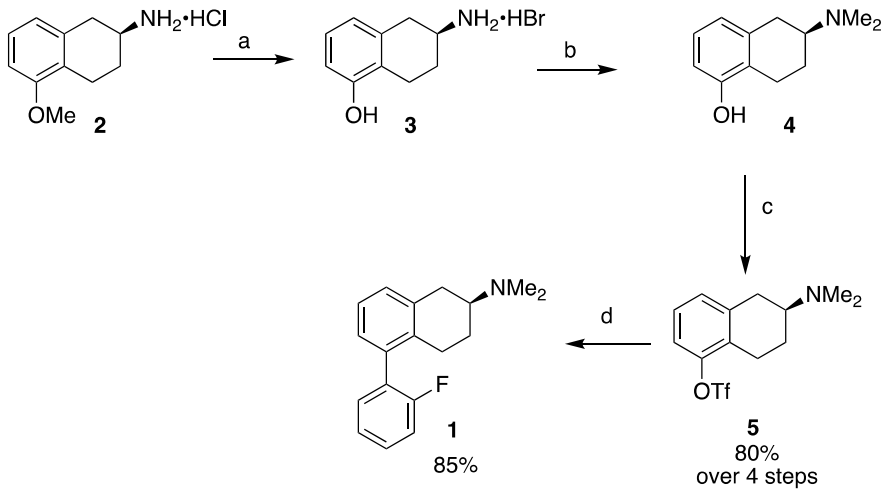

[a]Reagents and conditions: (a) 48% HBr aq, 130 °C, 3h; (b) CH_2O, MeOH, reflux, 2 h then $NaBH_4$, rt, 3 h; (c) N-(2-Pyridyl)-bis (trifluoromethanesulfonimide), DIPEA, CH_2Cl_2, –78 °C to rt, 20 h; (d) 2-Fluorophenylboronic acid, $Pd(PPh_3)_4$, K_3PO_4, KBr, dioxane, 120 °C, 6 h.

Scheme S1: Chiral synthesis of (*S*)-5-(2′-Fluorophenyl)-*N*,*N*-dimethyl-1,2,3,4-tetrahydronaphthalen-2-amine, **1 (FPT)** was based on Holmberg et al, 2004[1]. Commercially available (*2S)*-5-methoxy-2-aminotetralin hydrochloride **2** was demethylated under acidic conditions (48% HBr (aq)) to give (*2S)*-5-hydroxy-2-aminotetralin hydrobromide **3**. Modified Eschweiler-Clarke reaction (1) was employed to convert the primary amine **3** to (*2S)*-5-hydroxy-2-dimethylaminotetralin **4**, which was subsequently treated with *N*-(2-pyridyl)bis(trifluoromethanesulfonimide) under basic conditions to give intermediate triflate **5** in 80% yield over 4 steps from amine **2**. Finally, the Suzuki-Miyaura cross coupling of triflate **5** was performed with 2-F-phenylboronic acid **6** to afford (*S*)-5-(2′-Fluorophenyl)-*N*,*N*-dimethyl-1,2,3,4-tetrahydronaphthalen-2-amine **1** in 85% isolated yield.

Figure S5. FPT purity confirmed by HPLC. Results from LabSolutions show a single peak corresponding to the retention time of FPT.

Sample Name	: FPT		
Sample ID	:		
Data Filename	: Purity Test 2S-2'-F002.lcd		
Method Filename	: 2mL Method.lcm		
Batch Filename	:		
Vial #	: 1-1	Sample Type	: Unknown
Injection Volume	: 20 uL		
Date Acquired	: 5/23/2018 11:00:47 AM	Acquired by	: System Administrator
Date Processed	: 7/5/2019 2:13:21 PM	Processed by	: System Administrator

<Chromatogram>

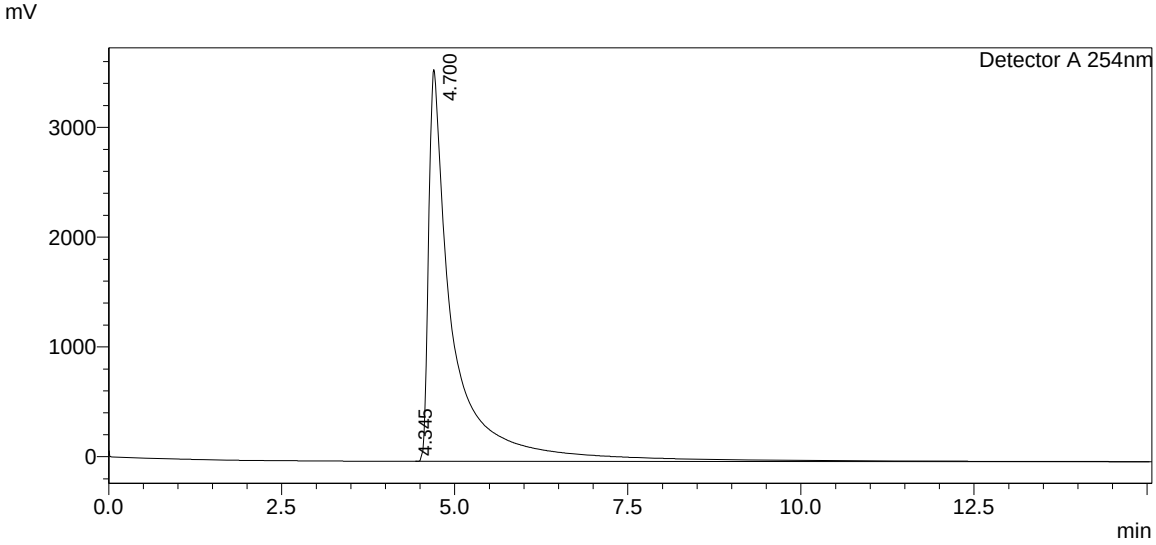

<Peak Table>

Detector A 254nm

Peak#	Ret. Time	Area	Height	Unit	Mark	Name	Area%
1	4.345	2899	398				0.003
2	4.700	89120863	3567322		V		99.997
Total		89123762	3567720				100.000

Picture S1. Representative example of the effect of FPT on marble-burying in *Fmr1* knockout (KO) and wild-type (WT) mice, relative to vehicle (Veh).

Analysis of Dissociation and Association Kinetics

The dissociation rate of [^{3}H]5-CT at 5-HT$_{1A}$Rs and 5-HT$_7$Rs was determined by fitting cpm values to a one-phase exponential decay model. If data points within the curve were smaller than the minimum binding at 180 minutes, or larger than the maximum at 1-minute timepoints, they were excluded from analysis (5 out of 480 data points for 5-HT$_7$Rs, and 15 out of 280 for 5-HT$_{1A}$Rs). Dissociation kinetics were not determined separately for 5-HT$_{2C}$Rs, but instead were determined alongside association parameters wherein three concentrations of radiolabel were globally fit using the association kinetics; two or more concentrations of hot ligand model using 12 timepoints. This model yielded best-fit values for k_{on} and k_{off} wherein the k_{off} was comparable to those determined via dissociation rate experiments at 5-HT$_{1A}$Rs and 5-HT$_7$Rs, and thus were pooled together in the final analysis. The k_{on} and k_{off} of FPT were determined by fitting the data to a kinetics of competitive binding model based on[2, 3]. One data point was excluded from 5-HT$_{1A}$R and two from 5-HT$_7$R association kinetics analysis (out of 144 points each) due to specific cpm values less than nonspecific binding. For FPT competitive kinetics, 12, 1, and 4 data points were excluded from analysis of FPT competition kinetics at 5-HT$_{1A}$Rs, 5-HT$_{2C}$Rs, and 5-HT$_7$Rs, respectively, for reasons outlined above. The models used to calculate kinetic values were based on the following equations:

$$K_A = k_1[L] + k_2$$

$$K_B = k_3[I] + k_4$$

$$K_F = 0.5[(K_A + K_B + \sqrt{(K_A - K_B)^2 + 4k_1k_3[L][I]})]$$

$$K_S = 0.5[(K_A + K_B - \sqrt{(K_A - K_B)^2 + 4k_1k_3[L][I]})]$$

$$Y = \frac{B_{max}\, k_1[L]}{K_F - K_S}\left[\frac{k_4(K_F - K_S)}{K_F K_S} + \frac{(k_4 - K_F)}{K_F}\exp(-K_F t) - \frac{(k_4 - K_S)}{K_S}\exp(-K_S t)\right]$$

$k_1 = k_{on}$ of radiolabel; $k_2 = k_{off}$ of radiolabel

$k_3 = k_{on}$ of FPT; $k_4 = k_{off}$ of FPT

L is the concentration of radioligand.

I is the concentration of FPT.

Y is specific binding in counts per minute (cpm)

B_{max} is the total binding in cpm, and t is time in minutes.

c-Fos Immunohistochemistry

Adult mice were deeply anesthetized with isoflurane and placed on their backs on ice. Mice were then perfused transcardially with 0.001% heparin, 0.9% saline solution, followed by 4% paraformaldehyde (PFA) in 0.05M phosphate buffered saline (PBS, pH 7.4). Perfusion flow was maintained at 40mL/min using a peristaltic pump. Brains were extracted and post-fixed in 4% PFA in 0.05 M PBS (pH 7.4) at 4°C for 24 hours. Brains were then transferred to 20% glycerol in 0.1 M PBS and stored at 4°C for 24-64 hours. Fifty µm coronal slices were sectioned in a cryostat (Leica CM1950, Leica Biosystems Inc., IL, USA) at a chamber temperature of -28°C and object head temperature of -26°C. Alternate sections were used for c-Fos or Nissl staining with cresyl violet acetate.

For c-Fos, sections were immediately transferred to 0.05M tris buffered saline (TBS) in plastic wells with mesh inserts. Sections were washed in TBS a minimum of four times, and washes with TBS were performed after each of the following incubation steps. Sections were transferred to a vial containing 10mM sodium citrate buffer (2.94 g trisodium citrate dihydrate and 0.5 ml Tween 20 in 1000 ml dH_2O, pH 6.0) at 85°C for 20 minutes. Sections were then incubated with 2% normal horse serum (NHS), 0.4% Triton X-100 (TX) in TBS. Sections were incubated in Bloxall® Blocking solution (SP-6000, Vector

Laboratories Inc., Burlingame, CA, USA) for 10 minutes. Sections were incubated with c-Fos antibody (1:1000 mouse monoclonal [2H2], Abcam ab208942, Cambridge, UK) in 1% NHS/0.4% TX/ 0.05 M TBS at 4°C overnight. Sections were incubated in secondary antibody (1:200 biotinylated anti-mouse IgG, Vectastain® Elite ABC Kit, Mouse IgG, Vector Laboratories Inc., Burlingame, CA, USA) in 1% NHS/0.2% TX/0.05 M TBS for 1 hour. Sections were incubated in ABC reagent (Vectastain® Elite ABC Kit, Mouse IgG, Vector Laboratories Inc., Burlingame, CA, USA) in 1% NHS/0.2% TX/TBS for 30 min. Sections were stained using 3,3'-diamobenzidine (DAB Substrate Kit 34002, Thermo Scientific, IL, USA). After washing in diluted TBS (0.01 to 0.005 M), sections were slide mounted. Sections were dehydrated using increasing concentrations of ethanol, cleared using Histoclear and then cover-slipped with DPX.

Cover-slipped slides were dried for at least 24 hours before visualization on Echo Revolve (Discover Echo, San Diego, CA, USA). For imaging the regions of interest, Allen Brain Reference Atlas was used. All sections were imaged at 46% light intensity. Brightness, contrast and color balance for c-Fos were in the ranges of 35-50, 70-80 and 10-45, respectively and for Nissl bodies, 45, 50 and 60, respectively. Imaged sections were first analyzed for counting c-Fos+ nuclei and then representative raw images were selected and adjusted for brightness, contrast and color balance in ImageJ software (ImageJ 1.52a Java; 1.8.0_112 [64-bit]). Scale was set using calibrated images—1.3309 pixels/micron for 4x images and 6.4910 pixels/micron for 20x images. Paintbrush tool was used to outline the regions of interest in BLA 4x image.

REFERENCES

1. Holmberg, P., Sohn, D., Leideborg, R., Caldirola, P., Zlatoidsky, P., Hanson, S., Mohell, N., Rosqvist, S., Nordvall, G., Johansson, A. M., and Johansson, R. (2004) Novel 2-aminotetralin and 3-aminochroman derivatives as selective serotonin 5-HT7 receptor agonists and antagonists, *J Med Chem 47*, 3927-3930.

2. Sykes, D. A., Bradley, M. E., Riddy, D. M., Willard, E., Reilly, J., Miah, A., Bauer, C., Watson, S. J., Sandham, D. A., Dubois, G., and Charlton, S. J. (2016) Fevipiprant (QAW039), a Slowly Dissociating CRTh2 Antagonist with the Potential for Improved Clinical Efficacy, *Mol Pharmacol 89*, 593-605.
3. Motulsky, H. J., and Mahan, L. C. (1984) The kinetics of competitive radioligand binding predicted by the law of mass action, *Mol Pharmacol 25*, 1-9.